

Review

# Modeling Arrhythmia in a Dish: An Open View from Human-Engineered Heart Constructs

Shiya Wang<sup>1,†</sup>, Pengcheng Yang<sup>1,2,†</sup>, Jonathan Nimal Selvaraj<sup>1,\*</sup> and Donghui Zhang<sup>1,3,\*</sup>

<sup>1</sup> State Key Laboratory of Biocatalysts and Enzyme Engineering, Stem Cells and Tissue Engineering Manufacture Center, School of Life Sciences, Hubei University, Wuhan 430062, China

<sup>2</sup> Biomanufacturing Center, Department of Mechanical Engineering, Tsinghua University, Beijing 100084, China

<sup>3</sup> Cardiovascular Research Institute, Union Hospital, Tongji Medical College, Huazhong University of Science and Technology, Wuhan 430022, China

\* Correspondence: jonathanimals@hubu.edu.cn (J.N.S.); donghui.zhang@hubu.edu.cn (D.Z.)

† These authors contributed equally to this work.

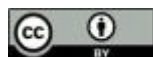
Received: 26 July 2024; Revised: 29 September 2024; Accepted: 30 September 2024; Published: 6 February 2025

**Abstract:** Human-engineered heart constructs (hEHC), comprising cardiac organoids and engineered heart tissues, have become essential for replicating pathological and physiological mechanisms associated with cardiac development and diseases. The ongoing advancements in fabrication and culture techniques for these constructs have rendered them increasingly vital for cardiotoxicity prediction and drug efficacy evaluations. There is an escalating demand for standardized methodologies encompassing uniform fabrication, accurate disease modeling, and multidimensional phenotype assessments to facilitate a comprehensive understanding of these constructs. This review systematically examines hEHC, highlighting recent advancements in their cellular composition and functional characteristics, while stressing the necessity for thorough evaluations of significant heart disease phenotype, particularly in arrhythmia. Here, we propose a novel modular classification of cardiac model development based on specific modeling parameters and categorize existing research on in vitro functional assessment into various quantitative metrics. This classification framework provides researchers with innovative insights and strategies for personalized model design and evaluation.

**Keywords:** tissue engineering; human-engineered heart construct; disease modeling; drug development; arrhythmia

## 1. Introduction

The heart is the first functional organ in the human embryo, garnering extensive interest in its development during embryogenesis and lifelong electrophysiological-mechanical coupling despite heart disease or aging. Various animal models have been utilized to explore the mysteries behind heart development and related diseases [1]. Still, these models pose challenges in elucidating mechanisms due to notable disparities in ion channels, membrane potential, and cardiac contraction frequency between animals and humans [2]. Additionally, primary adult human cardiomyocytes and engineered cells designed with specific ion channels for pharmacological testing inadequately represent the holistic efficacy of cardiac medications, primarily due to lacking intricate three-dimensional (3D) structures and functional characteristics of the myocardium [3,4]. The advent of human pluripotent stem cells (hPSC), including embryonic stem cells (hESC) and induced pluripotent stem cells (hiPSC), offers immense potential for advancing in vitro drug screening [5], developmental research, and regenerative medicine. Leveraging patient-derived hiPSC with specific genotypes and gene editing techniques facilitates the development of personalized human disease models to understand individual genotypes better and evaluate functional



**Copyright:** © 2025 by the authors. This is an open access article under the terms and conditions of the Creative Commons Attribution (CC BY) license (<https://creativecommons.org/licenses/by/4.0/>).

**Publisher's Note:** Scilight stays neutral with regard to jurisdictional claims in published maps and institutional affiliations.

recovery. These *in vitro* models can address the intrinsic limitations of animal models, such as ethical concerns [6] and interspecies variability [7], and contribute to a better understanding of cardiac development and disease, ultimately tackling cardiovascular disease, the leading cause of global mortality [8].

The continuous enhancement of differentiation protocols for directing hPSCs into various types of human cardiac cells, such as cardiomyocytes (CM) [9,10], cardiac fibroblasts (FB) [11,12], and endothelial cells (ED) [13,14], has significantly advanced the development of *in vitro* human cardiac models. With the availability of human cardiac cells, the primary focus of human heart engineering has transitioned to fabricating cardiac tissue. Currently, two dominant *in vitro* heart models effectively replicate the heart's cellular composition and physiological function: self-assembled cardiac spheroids and directionally assembled cardiac tissue. These models are collectively referred to as human-engineered heart constructs (hEHC) [15,16]. hEHC was selected as an overarching term over alternatives like cardiac organoid, cardiac microtissues, engineered heart tissue, or cardiopatches, as both self-assembled and directionally assembled approaches strive to utilize engineering technologies to orchestrate cardiac cells in forming synergistically tissue that partially mimics the heart's structure and function.

The self-assembled hEHC shows increased structural heterogeneity under various stimuli and provides significant advantages in delineating early cardiogenesis and the multicellular interactions associated with congenital heart disease. Zhen Ma et al. pioneered the generation of 3D hEHC featuring a central CM core and outer FB perimeter and predominantly comprising cell-free microchambers [17,18]. Drakhlis et al. advanced hEHC complexity by embedding hPSC-derived embryoid bodies in Matrigel to form a myocardium including cavities, as well as an inner core expressing anterior foregut endoderm markers SOX2, and an outer layer expressing posterior foregut endoderm markers like HNF4 $\alpha$  and PDX1 [19]. In contrast, the multicellular hEHC fabricated mainly through the directed assembly of cardiac cells, aimed to replicate certain electromechanical properties of adult myocardium *in vitro*. Selecting the most pertinent hEHC system—encompassing manufacturing strategies, genetic/non-genetic modeling factors, and functional assessment parameters—is paramount for cardiac-related investigations. Hence, this review elaborates on the evolutionary trajectory of hEHC over the past two decades, aiming to consolidate methodologies to effectively enhance the complexity and maturity of hEHC. Additionally, the representative application of hEHC in modeling arrhythmia, a prevalent phenotype associated with heart disease and drug-induced cardiotoxicity was highlighted, to ultimately advocate for a modular, multidimensional approach to constructing hEHC-based cardiac disease models.

## **2. Striving for Excellence: For More Mature and Complex hEHC**

The heart is a highly sophisticated organ that continuously pumps blood to deliver oxygen and nutrients via the circulatory system. This complexity poses challenges for *in vitro* models attempting to replicate the intricate architecture and electromechanical coupling of the myocardium. In 1960, Harary's team discovered that rat heart cells could self-aggregate to form beating fiber-like heart tissue *in vitro* [20]. This self-assembly property led to the initial cultivation of rat heart cells capable of producing defined, beating masses known as “mini-hearts” in the 1970s [21]. Concurrently, embryonic chick heart cells were cultured on an oriented substrate to form aligned muscle cell cores enveloped by an outer sheath of FB-like cells, also called cardiac muscle strands or bundles [22], thus laying the groundwork for heart tissue engineering. By the 1990s, Thomas's group developed a 3D collagen-based heart muscle model system [23], formally establishing the notion of engineered heart tissue in 2000 [24]. Undeniably, CM are the protagonists in executing the heart's function, comprising approximately 70% of the myocardial volume but only 20–30% of the total cellular composition [25,26]. The remaining 70% consists of interstitial cells such as FB, ED, epicardial cells (EP), and immune cells, which play indispensable roles in maintaining myocardial structure and functionality [27,28].

The initial impetus for introducing additional cells into hEHC was to improve their angiogenic capabilities in defective myocardial areas. In 2007, Oren et al. pioneered vascularized hEHC by introducing hESC-derived cardiomyocytes (hESC-CM), endothelial cells (hESC-ED), and embryonic FB into the poly L-lactic acid/polylactic glycolic acid scaffolds [29]. The integration of hESC-EC significantly enhanced vascularization and CM proliferation, while FB bolstered both the ED survival and proliferation capacity

within hEHC [29]. In parallel, adding ED and FB not only augmented the passive mechanical force of the hEHC but also enhanced its capacity to generate myocardium and microvessels post-implantation in rodent hearts [30]. In 2013, Donghui et al. first investigated the impact of these additional cells on hEHC's electromechanical characteristics, revealing that higher purities of CM (SIRPA<sup>+</sup> cells >90%) increased conduction velocities (up to 25.1 cm/s), although individual CM contractile force decrease [31]. To optimize hEHC design, Nimalan et al. developed hEHC (including directly assembled microwire and self-assembling aggregates) of varying ratios of CM-to-FB (100%, 75%, 50%, and 25% of NKX2.5-GFP<sup>+</sup> CM, with the remainder comprising CD90<sup>+</sup> FBs) and discovered that a 75% CM ratio resulted in more stable architecture and improved sarcomere alignment. They noted that the absence of FB and FB-mediated tissue remodeling led to structural instability in hEHC, while an excess FB triggered fibrosis and spatial heterogeneity [32]. Additionally, hEHC subjected to uniaxial mechanical stresses exhibited mature myocardium gene expression and a conduction velocity comparable to that of a healthy human heart, contrasting with self-assembling hEHC [32] (Table 1).

To assess the influence of diverse interstitial cell types on remodeling and cellular dynamics within hEHC, Meredith et al. constructed hEHC incorporating four interstitial cell populations. They found that the interstitial cells with optimal extracellular matrix (ECM) remodeling capabilities, such as dermal FB, significantly enhance CM maturation and alignment in hEHC [33]. Tiburcy et al. developed a serum-free method for hEHC construction [34,35], confirming that a CM to FB ratio of 0.7:0.3 could maximize contractile forces. They further highlighted that adding TGF- $\beta$ 1 during the early consolidation phases of hEHC substantially improves functional outcomes via FB-mediated ECM remodeling. Introducing hESC-derived epicardial cells (hESC-EP) to hEHC also promoted structural compaction and functional maturation [36], attributed to their embryonic FB-like characteristics and elevated fibronectin synthesis [36]. Notably, epicardial-derived FB can serve as a reservoir for cyclic guanosine monophosphate (GMP), boosting cyclic adenosine monophosphate (AMP) levels in CM via connexin 43-mediated gap junctions, thereby promoting CM maturation in tri-cellular hEHC [37,38]. ED within hEHC secrete specialized ECM components, like laminin-521, bolstering hEHC contractility through paracrine PDGFR $\beta$  signaling [39] (Table 1). The quantifiable presence of defined non-cardiomyocytes (non-CM), particularly EP and FB, beneficial for advancing the hEHC structural and functional maturation [37,38,40,41]. Beyond integrating non-CM into hEHC to enhance overall maturation, there exist more straightforward strategies targeting CM to finally manifest the traits of adult myocardium in hEHC. Extending culturing time from one to three weeks [42], or utilizing the fatty-acid-enriched media [43], can effectively boost CM connectivity and mitochondrial function, achieving peak contractility of 30 mN/mm<sup>2</sup>, which is comparable to the 25–44 mN/mm<sup>2</sup> range observed in adult human myocardium [42]. Moreover, electrical stimulation [44,45] or mechanical stretching [46,47] can directly “train” the CM in hEHC to further mature. Noteworthy is the progressive increase of the electrical stimulation frequency from 2 Hz to 6 Hz, which enables CM to exhibit physiologic sarcomere length (2.2  $\mu$ m) and large, well-organized T-tubules [44]. Nonetheless, achieving adult-level CM maturation in hEHC presents considerable challenges [48], particularly the efforts to enhance the conduction velocity of electrical signaling to align with the 46.4 cm/s found in adult myocardium [49]. Additionally, contemporary hEHC lacks the intricate complexity inherent to the native heart, including the endocardial, epicardial, immune, and nervous systems [50]. Thus, a deeper understanding of the interactions between CM and non-CM, along with their modulation, will be pivotal in developing hEHC with enhanced CM maturity and a cellular composition and organizational structure closer to the adult heart.

**Table 1.** Characterization of representative hEHC.

Year	Assembly method	Shape	Size	Cell type and Percentage	Extracellular Matrix	Culture Days	Structural Characteristics	Functional Characteristics	Application	Abbreviation
2007 [29]	Self-assemble	Shapeless	Undefined	hPSC-CM: hPSC-EC: EmF = 1:1:1	Pure Matrigel	14 days	a) The presence of typical sarcomeric pattern, T-tubules, sarcoplasmic reticulum, desmosomes, and gap junctions.	a) Spontaneous synchronous contractions; b) Synchronous Ca <sup>2+</sup> transients; c) Positive and negative chronotropic responses.	Drug test	EmF: human embryonic fibroblasts
2009 [30]	Self-assemble	Patch	Undefined	hPSC-CM: HUVEC: NHDF = 2:2:1	Without exogenous matrix	8 days	a) Formation of human CD31-positive endothelial cell networks.	a) Electrical pacing frequency: 3 Hz; b) Passive mechanics: 7.9 ± 3.1 mN/mm <sup>2</sup> .	Transplantation	HUVEC: human umbilical vein endothelial cells; NHDF: neonatal human dermal fibroblasts
2013 [31]	Directly assemble	Patch	7 × 7 mm <sup>2</sup>	48–65% hPSC-CM	2 mg/mL Fibrin and 10% Matrigel	14 days	a) Reaching optimal sarcomere length measured in adult human cardiomyocytes, 2.09 ± 0.02 μm.	a) Maximum conduction velocities: 25.1 cm/s; b) Maximum contractile force, 3.0 ± 1.1 mN and 11.8 ± 4.5 mN/mm <sup>2</sup> ; c) Positive inotropy with isoproterenol administration: 1.7 ± 0.3-fold force increase.	Drug test	
2013 [32]	Directly assemble	Wire	6 × 1 mm <sup>2</sup>	hPSC-CM: hPSC-CF = 3:1	3.7 mg/mL Collagen I	7 days	a) Increased length and alignment of the myofibrils and sarcomeres; b) Presence of Z disks and H zones.	a) Electrophysiological maturation: Excitation threshold: 2 V/CM; b) Maximum capture rate: 6 Hz; c) Conduction velocity: 47 cm/s.	Disease modeling	hPSC-CF: hPSC derived cardiac fibroblasts
2016 [33]	Directly assemble	Wire	17 × 3 mm <sup>2</sup>	hPSC-CM: HDF = 1:1	6 mg/mL Collagen I	14 days	a) Organized striated α actinin with 1.8 μm sarcomere lengths; b) Improvement in tissue compaction and homogeneity.	a) Peak contractile force: 0.1 mN/mm <sup>2</sup> ; b) Maximum capture rate: 2 Hz.	None	HDF: human dermal fibroblasts
2017 [35]	Directly assemble	Ring	Inner diameter 500 μm Outer diameter 1 μm	hPSC-CM: HFF = 7:3	0.8 mg/mL Collagen I	14 days	a) Sarcomere size: 1.93 μm; b) CM aspect ratio: 7.6; c) Sarcomere organization with clearly distinguishable Z-, I-, A-, H-, and M-bands.	a) Peak contractile force: 6.2 ± 0.8 mN/mm <sup>2</sup> ; b) Maximum capture rate: 3 Hz; c) Norepinephrine-induced heart failure.	Disease modeling	HFF: human foreskin fibroblasts
2017 [42]	Directly assemble	Patch	40 × 40 mm <sup>2</sup>	hPSC-CM: hPSC-CF = 8:2	2 mg/mL Fibrin and 10% Matrigel	21 days	a) Organized sarcomeres with H-zones, I-bands, M-bands, and Z-discs; b) T-tubule-like structures adjacent to Z-discs; c) Abundant mitochondria with well-developed cristae.	a) Active forces of contraction: 17.5 ± 1.1 mN and 17.0 ± 0.8 mN/mm <sup>2</sup> ; b) Conduction velocity: 28.9 ± 1.8 cm/s; c) Action potential duration at 80% repolarization: 471 ± 31 ms.	Transplantation	

**Table 1.** Continued.

Year	Assembly method	Shape	Size	Cell type and Percentage	Extracellular Matrix	Culture Days	Structural Characteristics	Functional Characteristics	Application	Abbreviation
2018 [44]	Directly assemble	Wire	6 × 2 mm <sup>2</sup>	hPSC-CM: HDF = 3 : 1	12 mg/mL Fibrinogen	28 days	a) Sarcomere length: 2.2 μm; b) Orderly registers of sarcomeres with I/A-bands, M-lines, Z-lines, desmosomes, intercalated discs; c) High density of mitochondria positioned adjacent to the contractile machinery; d) Robust t-tubules were co-localized with calcium handling proteins.	a) Resting membrane potential: -70 ± 2.7 mV; b) Conduction velocity: 25 ± 0.9 cm/s; c) Average contractile force: 3 mN/mm <sup>2</sup> ; d) Switch to oxidative metabolism.	Disease modeling	
2019 [45]	Directly assemble	Wire	3.5×0.5 mm <sup>2</sup>	hPSC-CM: HACF= 10 : 1	3.0mg/mL Collagen I and 15% Matrigel	21 days	a) Uniform longitudinal alignment of sarcomeric.	a) Conduction velocity: 5.7±0.9 cm/s in atrial tissue and 31.8±7.9 cm/s in ventricular tissue; b) Minimum diastolic potential: -70 mV; c) Upstroke velocities of action potential: 110 mV/ms; d) Differential response of atrial and ventricular tissue to drugs.	Disease modeling	HACF: Human adult cardiac fibroblasts
2019 [36]	Directly assemble	Wire	5×2 mm <sup>2</sup>	hPSC-CM: hPSC-EP=10 : 1	1.25 mg/mL Collagen I and 11% Geltrex	14 days	a) Aligned sarcomeric organization with 1.7 μm sarcomere length; b) Increased expression of connexin 43.	a) Peak contractile force: 0.03 mN; b) More rapid Ca <sup>2+</sup> -release and Ca <sup>2+</sup> -decay.	Transplantation	hPSC-EP: hPSC derived epicardial cells
2020 [37]	Self-assemble	Sphere	0.4 mm diameter	hPSC-CM: hPSC-FB: hPSC-EC= 14 : 3 : 3	Without exogenous matrix	21 days	a) Presence of caveolae, elongated and enlarged mitochondria with complex cristae; b) Organized sarcomeres with regular Z-lines, I-bands, H-zones, M-lines, and T-tubule-like structures	a) More negative resting membrane potentials and increased action potentials amplitudes; b) Higher contraction velocities; c) Greater amplitude of caffeine-induced Ca <sup>2+</sup> transients; d) Higher mitochondrial respiration and decreased dependence on glycolysis	Disease modeling	
2023 [39]	Directly assemble	Wire	1.6×0.6 mm <sup>2</sup>	hPSC-CM: hPSC-EC: HFCE= 3 : 1 : 1	2.6 mg/mL collagen I and 9% Matrigel	14 days	a) Increased organizational compaction; b) Increased ratios of MYH7/6 and MYL2/MYL7.	a) Contractile force: 250–500 μN correlates with 30–60 mN/mm <sup>2</sup> ; b) Endothelin-1 induced diastolic dysfunction.	Disease modeling	HFCE: Human fetal cardiac fibroblasts

### 3. Spin Silk from Cocoons: Arrhythmia in hEHC-Based Cardiac Disease Modeling

Cardiac arrhythmia is an irregular heart rate caused by various diseases such as myocardial infarction, diabetic cardiomyopathy, and congenital heart disease, potentially leading to heart failure [51]. Additionally, drug toxicity and conditions such as myocarditis can also cause life-threatening ventricular arrhythmias [52,53]. These conditions are all characterized by disorganized electromechanical coupling from fibrotic scar, particularly in the ventricular myocardium, which may result in sudden death in severe cases. Due to their significant risk and unpredictability, the diagnosis and pathogenesis of arrhythmias have consistently been research hotspots [54, 55]. Early afterdepolarization (EAD) is crucial in the onset of Long-QT syndrome (LQTS) and can lead to life-threatening Torsade de Pointes (TdP) arrhythmia. When assessing the effects of pharmacological agents or gene mutations related to LQTS on the EAD frequency, hEHC showed similar action potential characteristics and reverse use-dependence to adult left ventricular myocardium, unlike guinea pigs or rabbit models [56]. Nonetheless, the diminished coupling of CM in hEHC, due to relatively lower cellular density, alongside increased calcium influx from the immature hPSC-CM, predisposes them to a higher susceptibility to arrhythmic triggers than LV [56,57]. This susceptibility difference was also found between atrial CM-derived hEHC and ventricular CM-derived hEHC, where only atrial-hEHC showed spontaneous single or multiple spiral-wave reentrant loops. These electrophysiological reentrants can be rescued to normal rhythm by anti-arrhythmic drugs [58]. Notably, Masahide et al. first visualized the occurrence of reentrants characterized by featuring a meandering spiral wave center, exemplifying polymorphic ventricular tachycardia in hEHC. They proved that the accentuation of the 3D heterogeneity mediated by non-CM within hEHC is a prerequisite for the manifestation of TdP-like arrhythmias [59] (Table 2).

Arrhythmogenic cardiomyopathy patient-derived hiPSC-FB carrying the PKP2 mutation, but not the corresponding hiPSC-CM, significantly impaired the capacity of hEHC to capture high-frequency stimuli, thereby promoting an arrhythmic phenotype [37]. Furthermore, hEHC fabricated from LQTS patient-derived hPSC-CM (LQTS-CM) or FB (LQTS-FB) exhibited a prolonged action potential duration compared to normal hEHC, but both were shorter than that in hEHC fabricated using both LQTS-CMs and LQTS-FBs, indicating that the synergistic interaction between disease-type FB and CM contributes to a more realistic representation of LQTS characteristics [60]. The electrical coupling between FB and CM plays a vital role in cardiac excitability and arrhythmogenesis in animal models [61, 62], which undoubtedly provides solid theoretical insights to the further clarification of the non-CM composition of hEHC, particularly the highly heterogeneous FB and their interactions with CM during disease progression. The reticular structures formed by EC in self-assembled hEHC generated anisotropic stress gradients, resulting in the formation of multiple chambers within hEHC. Utilizing a micro-physiological system that simultaneously evaluates oxygen consumption, extracellular field potentials, and contraction of these multicellular hEHC, Mohammad et al. found that mitochondrial calcium oscillations triggered by MCU genetic deletions can induce arrhythmias [63] (Table 2). Additionally, optogenetic-based chronic intermittent tachypacing [64] and cryoinjury [65] also can serve as reproducible non-genetic arrhythmic triggers. When weakened the goal of mimicking tissue-level arrhythmias such as reentry, the self-assembled, micro hEHC (approximately 400  $\mu\text{m}$  diameter) exhibits greater batch stability for large-scale fabrication and assessment of action potential properties via optical mapping in response to various drugs [66], but of course, this miniaturization compromises CM maturation and electromechanical coupling heterogeneity across spatial dimensions, as illustrated by Kenneth et al. using a dual-camera to characterize the varying calcium signals on the upper and lower surfaces of directionally assembled arrhythmic hEHC [67]. The choice between prioritizing the number of assessment subjects using self-assembled hEHC versus the quality of assessment outcomes using directionally assembled hEHC to predict potential arrhythmic risk from genetic or non-genetic factors is like two sides of the same coin.

**Table 2.** Characterization of representative hEHC-based arrhythmia models.

Year	Assembly Method	Shape	Size	Cell type and Percentage	Extracellular Matrix	hEHC Construction Strategy	Culture Days	Triggers of Arrhythmia	Arrhythmia Characteristics	Disease Modeling	Abbreviations
2017 [59]	Self-assemble	Patch	6 × 6 mm	hPSC-CM: hPSC-mesenchymal cells = 1:1	Without exogenous matrix	Dissociated cells were recultured on temperature-responsive culture dishes to self-assemble hEHC.	3–21 days	100 nM E-4031 for 10 min with or without 1 Hz pacing.	a) Tachyarrhythmia: re-entry with a meandering pattern of the spiral wave center; b) FPD prolongation;	TdP arrhythmias	TdP: Torsade de Pointes; FPD: field potential duration.
2020 [37]	Self-assemble	Sphere	300 μm diameter	hPSC-CM: hPSC-cardiac FB: hPSC-EC = 14:3:3	Without exogenous matrix	Dissociated cells were seeded on V-bottom 96-well microplates and centrifuged to self-assemble hEHC.	21 days	The hPSC-FB from patient carrying the c.2013delC heterozygous mutation of the PKP2.	a) Reduce pacing capture percentage from 90% (1 Hz pacing), 80% (2 Hz pacing), 60% (3 Hz pacing) to 85%, 20%, 3%.	Arrhythmogenic cardiomyopathy	
2021 [66]	Self-assemble	Sphere	300 μm diameter	hPSC-CM: hCF = 19:1	Without exogenous matrix	Dissociated cells were added to the microwells with hemispherical bottoms to self-assemble hEHC.	6–8 days	a) 2 μM E4031 for 20 min; b) 100 μM ranolazine for 20 min; c) 1000 nM pollutant bisphenol A for 20 min.	a) Increased APD <sub>80</sub> from ~275 ms to ~650 ms; b) Increased APD <sub>80</sub> from ~250 ms to ~500 ms; c) Increased APD <sub>MaxR</sub> from ~280 ms to ~220 ms;	Drug cardiotoxicity	hCF: Primary normal adult human cardiac fibroblasts; APD <sub>80</sub> : action potential duration to 80%; APD <sub>MaxR</sub> : APD to the maximum repolarization rate.
2023 [63]	Self-assemble	Sphere	500 μm diameter	hPSC-CM: rat cardiac EC = 2:1	Matrigel	Dissociated cells were mixed in Matrigel and injected to PDMS microwells for self-assembling hEHC.	25 days	a) 10 μM KB-R7943 for 25 min; b) Mitochondrial calcium uniporter knocked out in hPSC-CM; c) 10 μM mitoxantrone for 70 min.	a) Decreased relative contractility, decreased relative potential amplitude, decreased oxygen oscillation amplitude;	Mitochondrial cardiomyopathy and drug cardiotoxicity	PDMS: Polydimethylsiloxane
2024 [60]	Self-assemble	Sphere	1.2 mm diameter	hPSC-CM: hPSC-cardiac FB: HUVEC = 2:1:1	2 mg/mL decellularized porcine heart extracellular matrix hydrogels	Dissociated cells were encapsulated in hydrogel to self-assemble hEHC.	21 days	The hPSC-CM and FB from LQTS patient carrying the 1264G>A, A422T mutation of the KCNH2.	a) LQTS-CM or LQTS-FB led to a FPD prolongation of hEHC from ~450 ms to ~550 ms.	Long QT Syndrome	HUVEC: human umbilical vein endothelial cells; LQTS: Long QT Syndrome; FPD: field potential duration.
2018 [56]	Directly assemble	Wire	1 mm × 200 μm	Undefined purity of hPSC-CM	5 mg/mL bovine fibrinogen and 10% Matrigel	Dissociated cells were mixed with hydrogels and pipetted into a 12 × 3 × 4 mm casting mold to directly assemble hEHC.	25–100 days	1 μM E-4031 for 15 min with 1 Hz pacing	a) Prolonged APD <sub>90</sub> from ~236 ms to ~517 ms; b) Triggered early after depolarizations in 50% of cases.	TdP arrhythmias	APD <sub>90</sub> : action potential duration to 90%;

**Table 2.** Continued.

Year	Assembly Method	Shape	Size	Cell type and Percentage	Extracellular Matrix	hEHC Construction Strategy	Culture Days	Triggers of Arrhythmia	Arrhythmia Characteristics	Disease Modeling	Abbreviations
2019 [57]	Directly assemble	Ring	Inner diameter 2.8 mm outer diameter 4.8 mm	> 85% cTNT+ hPSC-CM	10 mg/mL decellularized porcine heart tissue extracellular matrix hydrogels and 20% chitosan	Dissociated cells were combined with hydrogels and pipetted into circular casting molds to directly assemble hEHC.	30 days	a) The hPSC-CM from LQTS patient carrying A614V missense mutation of the KCNH2; b) The hPSC-CM from CPVT2 patient carrying D307H mutation of the CASQ2 treated with 10 μM isoproterenol or 2 Hz pacing; c) 100 μM lidocaine for 15 min with 1 Hz pacing	a) Prolonged APD <sub>90</sub> from ~200 ms to ~500 ms; b) Increased percentage of calcium transient abnormalities from 2.7% to 19%; c) Decreased conduction velocity from ~6 cm/s to ~3 cm/s.	Long QT Syndrome and CPVT	CPVT2: Catecholaminergic polymorphic ventricular tachycardia results from CASQ2 mutation;
2020 [64]	Directly assemble	Wire	6 × 1.3 mm	> 90% cTNT+ hPSC-CM	100 μg/mL Fibrinogen and 10% Matrigel	Dissociated cells were mixed with hydrogels and pipetted into a 12 × 3 × 4 mm casting mold to directly assemble hEHC. The hEHC was transduced with lentivirus expressing CHR2.	28 days	After 3 weeks of pacing at 3 Hz for 15 s followed by 15 s of no pacing to increase susceptibility, 20 Hz burst pacing was applied.	a) Increased incidence of tachycardia from 13% to 64%; b) Decreased APD <sub>90</sub> from ~160 ms to ~144 ms; c) Increased upstroke velocity from 43 V/s to 58 V/s.	Tachycardia	CHR2: channelrhodopsin-2;
2020 [58]	Directly assemble	Ring	Inner diameter 159 μm outer diameter 376 μm	> 90% cTnT <sup>+</sup> MLC2v hPSC-atrial CM	0.8 mg/mL Bovine Collagen Type I and 10% Matrigel	Dissociated cells were mixed with collagen and pipetted into circular molds to directly assemble hEHC. The hEHC was transferred onto passive silicon stretchers to contract.	undefined	hPSC-atrial CM	a) Re-entrant arrhythmias: a single circular re-entry wave; a single or multiple spiral-wave reentrant loops. b) Increased activation time from ~180 ms to ~280 ms.	Atrial fibrillation	
2021 [67]	Directly assemble	Wire	2.0 × 0.5 × 0.4 mm	hiPSC-CM: Hcf = 3:1	5 mg/mL fibrinogen and 10% Matrigel	Dissociated cells were mixed with hydrogels and pipetted into a microwell with two PDMS rods for directly assemble hEHC.	12 days	0.8 nM MBCD for 5 days.	a) Increased average wave front per frame from 0.2 to 1; b) Decreased conduction velocity from 18 cm/s to 0.6 cm/s; c) Decreased cycle length from 1000 ms to 500 ms; d) Decreased total length traveled by wavefront from 100% to 20%.	Drug cardiotoxicity	PDMS: Polydimethylsiloxane; MBCD: methyl-beta cyclodextrin.

#### 4. Where to Go Next: Accurate Modeling and Prediction

To develop an effective in vitro cardiac model for adaptation research and practical large-scale applications, four essential features need to be considered: (1) Using human-derived cellular components that are consistently sourced and produced under strict quality control; (2) Incorporating a 3D structure

resembling adult myocardium, which contains various cell types suitable for investigating cell interaction; (3) Including multiple measurable parameters related to clinical cardiac functionality; (4) Allowing integration with automated, high-throughput, and standardized testing. When developing hEHC-based arrhythmia models, prioritizing the enhancement of CM maturity and hEHC complexity is crucial. Adult CM do not exhibit spontaneous excitation and have dyad structures that swiftly react to membrane potential changes, thereby facilitating excitation-contraction coupling, indicating the higher presence of regulatory proteins in matured CM that maintain their stable resting membrane potential and support high levels of calcium homeostasis [68]. Consequently, advancing hEHC maturation minimizes false positives in the drug toxicity assessment [43] and diminishes the occurrence of irregular arrhythmia phenotypes in disease models [69]. Furthermore, the ion channel isoforms present in fetal-like CM mask the arrhythmic phenotype associated with mutations in adult myocardium isoforms, such as the *SCN5A* gene, which encodes the  $\alpha$ -subunit of the cardiac sodium channel Nav1.5, mutations in its adult exon 6 can trigger severe tachycardia and conduction disorders [70]. The multicellular composition that reflects the hEHC complexity also necessitates the consideration of multi-system interactions. For instance, integrating atria-like, atrioventricular canal-like, and ventricles-like hEHC can effectively replicate the heart's unidirectional conduction and "fast-slow-fast" activation pattern, inclusive of the associated atrioventricular conduction block [71]. Furthermore, the emergent concept of electroimmunology [51] underscores the essential role of immune cells in modulating myocardial electrophysiology in both physiological and pathological conditions. Macrophages, for example, can expedite CM repolarization through connexin-43 coupling, thereby enhancing electrical conduction within the atrioventricular node [72]. Additionally, exploring the influence of vagal and sympathetic nerve interactions on cardiac electrophysiological signals [73,74] based on multicellular and multi-system hEHC represents a promising and intriguing area of research. In light of the intricate system delineated above, additional priority is to dissect the disease into interconnected genetic and non-genetic factors for acute simulations (Figure 1), as heart diseases can stem from genetic and non-genetic interactions. Genetic factors can include mutations in functional genes and changes in non-coding regions. For cardiomyopathy, gene mutations in the cellular cytoskeleton, metabolism, and ion channels can lead to structural and functional abnormalities.

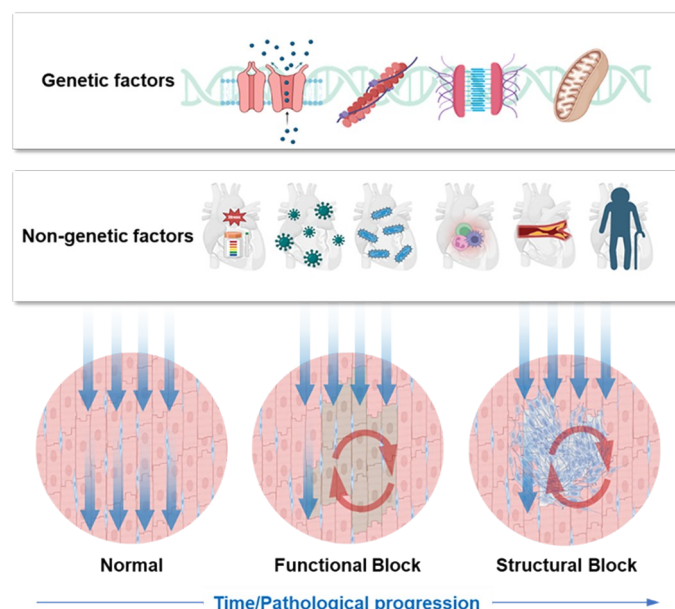


**Figure 1.** Myocardium arrhythmias induced by fibrotic scarring are common events in various heart diseases.

Multiple pathogenic factors, such as atherosclerosis, hyperglycemia, infections, and genetic alterations, prompt myocardial fibrosis via cardiac FB. The resultant dense fibrotic scar, lacking the electrophysiological characteristics akin to those of oriented myocardium, obstructs the consistent electrical signal propagation, causing localized conduction block or reentry. Concurrently, the FB at the margins of the fibrotic scar can

connect CM via synaptic or gap junctions, resulting in CM asynchronous activation, thereby heightening the susceptibility to arrhythmias. This arrhythmia phenotype can be replicated in hPSC-derived-hEHC. To benchmark the pathogenic factors causing arrhythmia, both unifactorial and multifactorial modeling approaches in hEHC, including drug cardiotoxicity, elevated glucose/lipid cultures, virus/bacterial infections, aging factor, and genetic modifications related to ion channel, mitochondrial, cytoskeleton, reveal varying degrees of electrophysiological abnormalities, including conduction blocks and reentry circuits, which, in turn, provides a valuable humanized platform for studying arrhythmogenesis and potential therapeutic targets.

Somatic cell reprogramming and gene editing techniques allow for generating cell lines with specific genotypes as patients, thereby further providing cardiac cells with targeted gene alterations. Meanwhile, non-genetic factors contributing to cardiac anomalies can include ischemia, metabolite induction, nutrient shortages, drugs, infections, and inflammation (Figure 1). hEHC-based heart disease models can integrate non-genetic factors through various culture conditions. A combined approach of genetic and non-genetic factors enables the development of multifactorial heart disease models, simulating significant secondary hit theories. In cases of drug withdrawal due to toxic effects exacerbating the arrhythmia phenotype, early detection of potential toxicity before preclinical trials can improve drug development efficiency and reduce cardiac-related mortality risk. Relying only on morphology, contraction amplitude, and molecular biology assessments may not be sufficient for detecting arrhythmic patterns in hEHC-based heart disease models. Therefore, emphasis should be placed on quantitatively correlating and forecasting electrical conduction characteristics of hEHC and related arrhythmia risk (Figure 2).

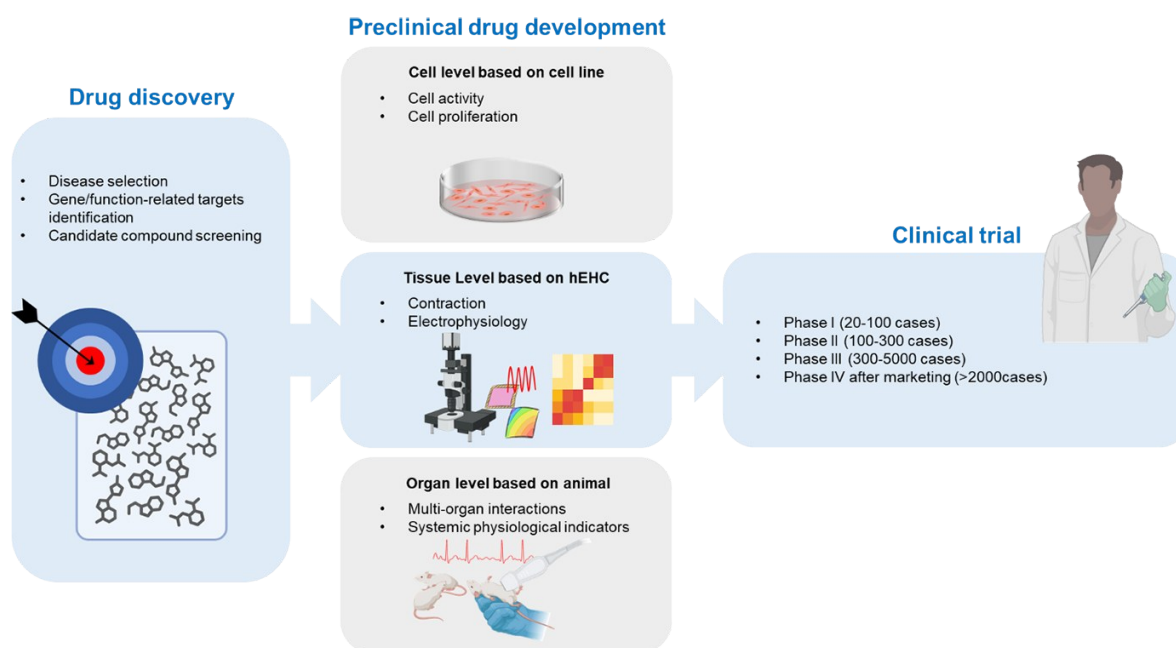


**Figure 2.** Accelerated preclinical drug development through multidimensional efficacy evaluation of compounds for arrhythmia risk reduction in hEHC.

Overall, the advancement of in vitro human cardiac models should focus on functional attributes dominated by various cardiac cells, especially advanced adult myocardium-level functions, rather than solely on CM fate determinations. Quantitatively understanding and forecasting electrical conduction properties alongside the arrhythmia risk in hEHC can be a significant focal point in the field of cardiac modeling.

The drug development process can be categorized into three primary periods: drug candidate discovery, preclinical drug development utilizing diverse models, and clinical trials involving varied patient demographics. Physiological or pathological models derived from hEHC can mitigate the limitations of cell models in functional characteristics observed at the myocardial level, while also tackling the species-specific differences between animals and humans. This hEHC approach facilitates the efficient screening of compound libraries and the identification of potential cardiotoxicity.

**Author Contributions:** S.W., P.Y., J.N.S. and D.Z. wrote the manuscript and organized the figure. All authors have read and agreed the published version of the manuscript.

**Funding:** D.Z. was funded by the National Key R&D Program of China (2021YFA1101902) and the National Natural Science Foundation of China (32171107).

**Institutional Review Board Statement:** Not applicable.

**Informed Consent Statement:** Not applicable.

**Data Availability Statement:** Not applicable.

**Acknowledgments:** Some of the drawings in Figure 1 and 2 were created in <https://BioRender.com>.

**Conflicts of Interest:** The authors declare that they have no known competing financial interests.

## References

1. Blackwell, D.J.; Schmeckpeper, J.; Knollmann, B.C. Animal Models to Study Cardiac Arrhythmias. *Circ. Res.* **2022**, *130*, 1926–1964. <https://doi.org/10.1161/CIRCRESAHA.122.320258>.
2. Clauss, S.; Bleyer, C.; Schuttler, D.; et al. Animal models of arrhythmia: Classic electrophysiology to genetically modified large animals. *Nat. Rev. Cardiol.* **2019**, *16*, 457–475. <https://doi.org/10.1038/s41569-019-0179-0>.
3. Zhou, B.; Shi, X.; Tang, X.; et al. Functional isolation, culture and cryopreservation of adult human primary cardiomyocytes. *Signal Transduct. Target. Ther.* **2022**, *7*, 254. <https://doi.org/10.1038/s41392-022-01044-5>.
4. Batista Napotnik, T.; Kos, B.; Jarm, T.; et al. Genetically engineered HEK cells as a valuable tool for studying electroporation in excitable cells. *Sci. Rep.* **2024**, *14*, 720. <https://doi.org/10.1038/s41598-023-51073-5>.
5. Liang, P.; Lan, F.; Lee, A.S.; et al. Drug screening using a library of human induced pluripotent stem cell-derived cardiomyocytes reveals disease-specific patterns of cardiotoxicity. *Circulation* **2013**, *127*, 1677–1691. <https://doi.org/10.1161/CIRCULATIONAHA.113.001883>.
6. Levy, N. The use of animal as models: Ethical considerations. *Int. J. Stroke* **2012**, *7*, 440–442. <https://doi.org/10.1111/j.1747-4949.2012.00772.x>.
7. Mukherjee, P.; Roy, S.; Ghosh, D.; et al. Role of animal models in biomedical research: A review. *Lab. Anim. Res.* **2022**, *38*, 18. <https://doi.org/10.1186/s42826-022-00128-1>.
8. Farzadfar, F. Cardiovascular disease risk prediction models: Challenges and perspectives. *Lancet Glob. Health* **2019**, *7*, e1288–e1289. [https://doi.org/10.1016/S2214-109X\(19\)30365-1](https://doi.org/10.1016/S2214-109X(19)30365-1).
9. Lian, X.; Zhang, J.; Azarin, S.M.; et al. Directed cardiomyocyte differentiation from human pluripotent stem cells by modulating Wnt/beta-catenin signaling under fully defined conditions. *Nat. Protoc.* **2013**, *8*, 162–175. <https://doi.org/10.1038/nprot.2012.150>.
10. Lian, X.; Bao, X.; Zilberter, M.; et al. Chemically defined, albumin-free human cardiomyocyte generation. *Nat. Methods* **2015**, *12*, 595–596. <https://doi.org/10.1038/nmeth.3448>.
11. Zhang, H.; Tian, L.; Shen, M.; et al. Generation of Quiescent Cardiac Fibroblasts From Human Induced Pluripotent Stem Cells for In Vitro Modeling of Cardiac Fibrosis. *Circ. Res.* **2019**, *125*, 552–566. <https://doi.org/10.1161/CIRCRESAHA.119.315491>.
12. Zhang, J.; Tao, R.; Campbell, K.F.; et al. Functional cardiac fibroblasts derived from human pluripotent stem cells via second heart field progenitors. *Nat. Commun.* **2019**, *10*, 2238. <https://doi.org/10.1038/s41467-019-09831-5>.
13. Paik, D.T.; Tian, L.; Lee, J.; et al. Large-Scale Single-Cell RNA-Seq Reveals Molecular Signatures of Heterogeneous Populations of Human Induced Pluripotent Stem Cell-Derived Endothelial Cells. *Circ. Res.* **2018**, *123*, 443–450. <https://doi.org/10.1161/CIRCRESAHA.118.312913>.
14. Wang, K.; Lin, R.-Z.; Hong, X.; et al. Robust differentiation of human pluripotent stem cells into endothelial cells via temporal modulation of ETV2 with modified mRNA. *Sci. Adv.* **2020**, *6*, eaba7606. <https://doi.org/10.1126/sciadv.aba7606>.
15. Cho, S.; Discher, D.E.; Leong, K.W.; et al. Challenges and opportunities for the next generation of cardiovascular tissue engineering. *Nat. Methods* **2022**, *19*, 1064–1071. <https://doi.org/10.1038/s41592-022-01591-3>.
16. Liu, C.; Feng, X.; Li, G.; et al. Generating 3D human cardiac constructs from pluripotent stem cells. *EBioMedicine* **2022**, *76*, 103813. <https://doi.org/10.1016/j.ebiom.2022.103813>.
17. Ma, Z.; Wang, J.; Loskill, P.; et al. Self-organizing human cardiac microchambers mediated by geometric confinement. *Nat. Commun.* **2015**, *6*, 7413. <https://doi.org/10.1038/ncomms8413>.
18. Hoang, P.; Wang, J.; Conklin, B.R.; et al. Generation of spatial-patterned early-developing cardiac organoids using human pluripotent stem cells. *Nat. Protoc.* **2018**, *13*, 723–737. <https://doi.org/10.1038/nprot.2018.006>.
19. Drakhlis, L.; Biswanath, S.; Farr, C.-M.; et al. Human heart-forming organoids recapitulate early heart and foregut development. *Nat. Biotechnol.* **2021**, *39*, 737–746. <https://doi.org/10.1038/s41587-021-00815-9>.
20. Harary, I.; Farley, B. In vitro Organization of Single Beating Rat Heart Cells into Beating Fibers. *Science* **1960**, *132*, 1839–1840. doi:doi:10.1126/science.132.3442.1839.
21. Halbert, S.P.; Bruderer, R.; Lin, T.M. In vitro organization of dissociated rat cardiac cells into beating three-dimensional structures. *J. Exp. Med.* **1971**, *133*, 677–695. <https://doi.org/10.1084/jem.133.4.677>.
22. Lieberman, M.; Roggeveen, A.E.; Purdy, J.E.; et al. Synthetic Strands of Cardiac Muscle: Growth and Physiological Implication. *Science* **1972**, *175*, 909–911. doi:doi:10.1126/science.175.4024.909.
23. Eschenhagen, T.; Fink, C.; Remmers, U.; et al. Three-dimensional reconstitution of embryonic cardiomyocytes in a collagen

- matrix: A new heart muscle model system. *FASEB J.* **1997**, *11*, 683–694. <https://doi.org/10.1096/fasebj.11.8.9240969>.
24. Zimmermann, W. H.; Fink, C.; Kralisch, D.; et al. Three-dimensional engineered heart tissue from neonatal rat cardiac myocytes. *Biotechnol. Bioeng.* **2000**, *68*, 106–114.
  25. Zhou, P.; Pu, W.T. Recounting Cardiac Cellular Composition. *Circ. Res.* **2016**, *118*, 368–370. <https://doi.org/10.1161/CIRCRESAHA.116.308139>.
  26. Guo, Y.; Pu, W.T. Cardiomyocyte Maturation: New Phase in Development. *Circ. Res.* **2020**, *126*, 1086–1106. <https://doi.org/10.1161/CIRCRESAHA.119.315862>.
  27. Forte, E.; Furtado, M.B.; Rosenthal, N. The interstitium in cardiac repair: Role of the immune-stromal cell interplay. *Nat. Rev. Cardiol.* **2018**, *15*, 601–616. <https://doi.org/10.1038/s41569-018-0077-x>.
  28. Forte, E.; Skelly, D. A.; Chen, M.; et al. Dynamic Interstitial Cell Response during Myocardial Infarction Predicts Resilience to Rupture in Genetically Diverse Mice. *Cell Rep.* **2020**, *30*, 3149–3163 e3146. <https://doi.org/10.1016/j.celrep.2020.02.008>.
  29. Caspi, O.; Lesman, A.; Basevitch, Y.; et al. Tissue engineering of vascularized cardiac muscle from human embryonic stem cells. *Circ. Res.* **2007**, *100*, 263–272. <https://doi.org/10.1161/01.RES.0000257776.05673.ff>.
  30. Stevens, K.R.; Kreutziger, K.L.; Dupras, S.K.; et al. Physiological function and transplantation of scaffold-free and vascularized human cardiac muscle tissue. *Proc. Natl. Acad. Sci. USA* **2009**, *106*, 16568–16573. <https://doi.org/10.1073/pnas.0908381106>.
  31. Zhang, D.; Shadrin, I.Y.; Lam, J.; et al. Tissue-engineered cardiac patch for advanced functional maturation of human ESC-derived cardiomyocytes. *Biomaterials* **2013**, *34*, 5813–5820. <https://doi.org/10.1016/j.biomaterials.2013.04.026>.
  32. Thavandiran, N.; Dubois, N.; Mikryukov, A.; et al. Design and formulation of functional pluripotent stem cell-derived cardiac microtissues. *Proc. Natl. Acad. Sci. USA* **2013**, *110*, E4698–E4707. <https://doi.org/10.1073/pnas.1311120110>.
  33. Roberts, M. A.; Tran, D.; Coulombe, K. L.; et al. Stromal Cells in Dense Collagen Promote Cardiomyocyte and Microvascular Patterning in Engineered Human Heart Tissue. *Tissue Eng. Part. A* **2016**, *22*, 633–644. <https://doi.org/10.1089/ten.TEA.2015.0482>.
  34. Yang, X.; Murry, C.E. One Stride Forward: Maturation and Scalable Production of Engineered Human Myocardium. *Circulation* **2017**, *135*, 1848–1850. <https://doi.org/10.1161/CIRCULATIONAHA.117.024751>.
  35. Tiburcy, M.; Hudson, J.E.; Balfanz, P.; et al. Defined Engineered Human Myocardium With Advanced Maturation for Applications in Heart Failure Modeling and Repair. *Circulation* **2017**, *135*, 1832–1847. <https://doi.org/10.1161/CIRCULATIONAHA.116.024145>.
  36. Bargehr, J.; Ong, L. P.; Colzani, M.; et al. Epicardial cells derived from human embryonic stem cells augment cardiomyocyte-driven heart regeneration. *Nat. Biotechnol.* **2019**, *37*, 895–906. <https://doi.org/10.1038/s41587-019-0197-9>.
  37. Giacomelli, E.; Meraviglia, V.; Campostrini, G.; et al. Human-iPSC-Derived Cardiac Stromal Cells Enhance Maturation in 3D Cardiac Microtissues and Reveal Non-cardiomyocyte Contributions to Heart Disease. *Cell Stem Cell* **2020**, *26*, 862–879.e11. <https://doi.org/10.1016/j.stem.2020.05.004>.
  38. Lou, X.; Tang, Y.; Ye, L.; et al. Cardiac muscle patches containing four types of cardiac cells derived from human pluripotent stem cells improve recovery from cardiac injury in mice. *Cardiovasc. Res.* **2023**, *119*, 1062–1076. <https://doi.org/10.1093/cvr/cvad004>.
  39. Voges, H.K.; Foster, S.R.; Reynolds, L.; et al. Vascular cells improve functionality of human cardiac organoids. *Cell Rep.* **2023**, *42*, 112322. <https://doi.org/10.1016/j.celrep.2023.112322>.
  40. Munawar, S.; Turnbull, I.C. Cardiac Tissue Engineering: Inclusion of Non-cardiomyocytes for Enhanced Features. *Front. Cell Dev. Biol.* **2021**, *9*, 653127. <https://doi.org/10.3389/fcell.2021.653127>.
  41. Floy, M. E.; Dunn, K. K.; Mateyka, T. D.; et al. Direct coculture of human pluripotent stem cell-derived cardiac progenitor cells with epicardial cells induces cardiomyocyte proliferation and reduces sarcomere organization. *J. Mol. Cell Cardiol.* **2022**, *162*, 144–157. <https://doi.org/10.1016/j.yjmcc.2021.09.009>.
  42. Shadrin, I. Y.; Allen, B. W.; Qian, Y.; et al. Cardiopatch platform enables maturation and scale-up of human pluripotent stem cell-derived engineered heart tissues. *Nat. Commun.* **2017**, *8*, 1825. <https://doi.org/10.1038/s41467-017-01946-x>.
  43. Huebsch, N.; Charrez, B.; Neiman, G.; et al. Metabolically driven maturation of human-induced-pluripotent-stem-cell-derived cardiac microtissues on microfluidic chips. *Nat. Biomed. Eng.* **2022**, *6*, 372–388. <https://doi.org/10.1038/s41551-022-00884-4>.
  44. Ronaldson-Bouchard, K.; Ma, S.P.; Yeager, K.; et al. Advanced maturation of human cardiac tissue grown from pluripotent stem cells. *Nature* **2018**, *556*, 239–243. <https://doi.org/10.1038/s41586-018-0016-3>.
  45. Zhao, Y.; Rafatian, N.; Feric, N.T.; et al. A Platform for Generation of Chamber-Specific Cardiac Tissues and Disease Modeling. *Cell* **2019**, *176*, 913–927.e18. <https://doi.org/10.1016/j.cell.2018.11.042>.
  46. Abilez, O. J.; Tzatzalos, E.; Yang, H.; et al. Passive Stretch Induces Structural and Functional Maturation of Engineered Heart Muscle as Predicted by Computational Modeling. *Stem Cells* **2018**, *36*, 265–277. <https://doi.org/10.1002/stem.2732>.
  47. Leonard, A.; Bertero, A.; Powers, J.D.; et al. Afterload promotes maturation of human induced pluripotent stem cell derived cardiomyocytes in engineered heart tissues. *J. Mol. Cell Cardiol.* **2018**, *118*, 147–158. <https://doi.org/10.1016/j.yjmcc.2018.03.016>.
  48. Zhang, D.; Pu, W.T. Exercising engineered heart muscle to maturity. *Nat. Rev. Cardiol.* **2018**, *15*, 383–384. <https://doi.org/10.1038/s41569-018-0032-x>.
  49. Durrer, D.; van Dam, R.T.; Freud, G.E.; et al. Total excitation of the isolated human heart. *Circulation* **1970**, *41*, 899–912. <https://doi.org/10.1161/01.cir.41.6.899>.

50. Drakhlis, L.; Zweigerdt, R. Heart in a dish—Choosing the right in vitro model. *Dis. Model. Mech.* **2023**, *16*, dmm049961. <https://doi.org/10.1242/dmm.049961>.
51. Grune, J.; Yamazoe, M.; Nahrendorf, M. Electroimmunology and cardiac arrhythmia. *Nat. Rev. Cardiol.* **2021**, *18*, 547–564. <https://doi.org/10.1038/s41569-021-00520-9>.
52. Tisdale, J.E.; Chung, M.K.; Campbell, K.B.; et al. Drug-Induced Arrhythmias: A Scientific Statement From the American Heart Association. *Circulation* **2020**, *142*, e214–e233. <https://doi.org/10.1161/CIR.0000000000000905>.
53. Peretto, G.; Sala, S.; Rizzo, S.; et al. Ventricular Arrhythmias in Myocarditis: Characterization and Relationships With Myocardial Inflammation. *J. Am. Coll. Cardiol.* **2020**, *75*, 1046–1057. <https://doi.org/10.1016/j.jacc.2020.01.036>.
54. Sepehri Shamloo, A.; Bunch, T.J.; Lin, Y.J.; et al. Risk Assessment in Cardiac Arrhythmias. *Eur. Heart J.* **2020**, *41*, 4455–4457. <https://doi.org/10.1093/eurheartj/ehaa808>.
55. Järvensivu-Koivunen, M.; Tynkkynen, J.; Oksala, N.; et al. Ventricular arrhythmias and haemodynamic collapse during acute coronary syndrome: Increased risk for sudden cardiac death? *Eur. J. Prev. Cardiol.* **2024**, zwae074. <https://doi.org/10.1093/eurjpc/zwae074>.
56. Lemoine, M.D.; Krause, T.; Koivumaki, J.T.; et al. Human Induced Pluripotent Stem Cell-Derived Engineered Heart Tissue as a Sensitive Test System for QT Prolongation and Arrhythmic Triggers. *Circ. Arrhythm. Electrophysiol.* **2018**, *11*, e006035. <https://doi.org/10.1161/CIRCEP.117.006035>.
57. Goldfracht, I.; Efraim, Y.; Shinnawi, R.; et al. Engineered heart tissue models from hiPSC-derived cardiomyocytes and cardiac ECM for disease modeling and drug testing applications. *Acta Biomater.* **2019**, *92*, 145–159. <https://doi.org/10.1016/j.actbio.2019.05.016>.
58. Goldfracht, I.; Protze, S.; Shiti, A.; et al. Generating ring-shaped engineered heart tissues from ventricular and atrial human pluripotent stem cell-derived cardiomyocytes. *Nat. Commun.* **2020**, *11*, 75. <https://doi.org/10.1038/s41467-019-13868-x>.
59. Kawatou, M.; Masumoto, H.; Fukushima, H.; et al. Modelling Torsade de Pointes arrhythmias in vitro in 3D human iPSC cell-engineered heart tissue. *Nat. Commun.* **2017**, *8*, 1078. <https://doi.org/10.1038/s41467-017-01125-y>.
60. Min, S.; Kim, S.; Sim, W.S.; et al. Versatile human cardiac tissues engineered with perfusable heart extracellular microenvironment for biomedical applications. *Nat. Commun.* **2024**, *15*, 2564. <https://doi.org/10.1038/s41467-024-46928-y>.
61. Pellman, J.; Zhang, J.; Sheikh, F. Myocyte-fibroblast communication in cardiac fibrosis and arrhythmias: Mechanisms and model systems. *J. Mol. Cell Cardiol.* **2016**, *94*, 22–31. <https://doi.org/10.1016/j.yjmcc.2016.03.005>.
62. Wang, Y.; Li, Q.; Tao, B.; et al. Fibroblasts in heart scar tissue directly regulate cardiac excitability and arrhythmogenesis. *Science* **2023**, *381*, 1480–1487. <https://doi.org/10.1126/science.adh9925>.
63. Ghosheh, M.; Ehrlich, A.; Ioannidis, K.; et al. Electro-metabolic coupling in multi-chambered vascularized human cardiac organoids. *Nat. Biomed. Eng.* **2023**, *7*, 1493–1513. <https://doi.org/10.1038/s41551-023-01071-9>.
64. Lemme, M.; Braren, I.; Prondzynski, M.; et al. Chronic intermittent tachypacing by an optogenetic approach induces arrhythmia vulnerability in human engineered heart tissue. *Cardiovasc. Res.* **2020**, *116*, 1487–1499. <https://doi.org/10.1093/cvr/cvz245>.
65. Hofbauer, P.; Jahnel, S.M.; Papai, N.; et al. Cardioids reveal self-organizing principles of human cardiogenesis. *Cell* **2021**, *184*, 3299–3317 e3222. <https://doi.org/10.1016/j.cell.2021.04.034>.
66. Kofron, C.M.; Kim, T.Y.; Munarin, F.; et al. A predictive in vitro risk assessment platform for pro-arrhythmic toxicity using human 3D cardiac microtissues. *Sci. Rep.* **2021**, *11*, 10228. <https://doi.org/10.1038/s41598-021-89478-9>.
67. Williams, K.; Liang, T.; Masse, S.; et al. A 3-D human model of complex cardiac arrhythmias. *Acta Biomater.* **2021**, *132*, 149–161. <https://doi.org/10.1016/j.actbio.2021.03.004>.
68. Lu, F.; Pu, W.T. The architecture and function of cardiac dyads. *Biophys. Rev.* **2020**, *12*, 1007–1017. <https://doi.org/10.1007/s12551-020-00729-x>.
69. Liang, W.; Gasparyan, L.; AlQarawi, W.; et al. Disease modeling of cardiac arrhythmias using human induced pluripotent stem cells. *Expert. Opin. Biol. Ther.* **2019**, *19*, 313–333. <https://doi.org/10.1080/14712598.2019.1575359>.
70. Campostrini, G.; Kosmidis, G.; Ward-van Oostwaard, D.; et al. Maturation of hiPSC-derived cardiomyocytes promotes adult alternative splicing of SCN5A and reveals changes in sodium current associated with cardiac arrhythmia. *Cardiovasc. Res.* **2023**, *119*, 167–182. <https://doi.org/10.1093/cvr/cvac059>.
71. Li, J.; Wiesinger, A.; Fokkert, L.; et al. Modeling the atrioventricular conduction axis using human pluripotent stem cell-derived cardiac assembloids. *Cell Stem Cell* **2024**. <https://doi.org/10.1016/j.stem.2024.08.008>.
72. Hulsmans, M.; Clauss, S.; Xiao, L.; et al. Macrophages Facilitate Electrical Conduction in the Heart. *Cell* **2017**, *169*, 510–522 e520. <https://doi.org/10.1016/j.cell.2017.03.050>.
73. Rajendran, P.S.; Hadaya, J.; Khalsa, S.S.; et al. The vagus nerve in cardiovascular physiology and pathophysiology: From evolutionary insights to clinical medicine. *Semin. Cell Dev. Biol.* **2024**, *156*, 190–200. <https://doi.org/10.1016/j.semedb.2023.01.001>.
74. Chen, W.G.; Schloesser, D.; Arensdorf, A.M.; et al. The Emerging Science of Interoception: Sensing, Integrating, Interpreting, and Regulating Signals within the Self. *Trends Neurosci.* **2021**, *44*, 3–16. <https://doi.org/10.1016/j.tins.2020.10.007>.